

Direct Measurement of the W Boson Width

V.M. Abazov³⁷, B. Abbott⁷⁵, M. Abolins⁶⁵, B.S. Acharya³⁰, M. Adams⁵¹, T. Adams⁴⁹, E. Aguilo⁶, M. Ahsan⁵⁹, G.D. Alexeev³⁷, G. Alkhalaf⁴¹, A. Alton^{64,a}, G. Alverson⁶³, G.A. Alves², L.S. Ancu³⁶, T. Andeen⁵³, M.S. Anzelc⁵³, M. Aoki⁵⁰, Y. Arnaud¹⁴, M. Arov⁶⁰, M. Arthaud¹⁸, A. Askew⁴⁹, B. Åsman⁴², O. Atramentov^{49,b}, C. Avila⁸, J. BackusMayes⁸², F. Badaud¹³, L. Bagby⁵⁰, B. Baldin⁵⁰, D.V. Bandurin⁵⁹, S. Banerjee³⁰, E. Barberis⁶³, A.-F. Barfuss¹⁵, P. Bargassa⁸⁰, P. Baringer⁵⁸, J. Barreto², J.F. Bartlett⁵⁰, U. Bassler¹⁸, D. Bauer⁴⁴, S. Beale⁶, A. Bean⁵⁸, M. Begalli³, M. Begel⁷³, C. Belanger-Champagne⁴², L. Bellantoni⁵⁰, J.A. Benitez⁶⁵, S.B. Beri²⁸, G. Bernardi¹⁷, R. Bernhard²³, I. Bertram⁴³, M. Besançon¹⁸, R. Beuselinck⁴⁴, V.A. Bezzubov⁴⁰, P.C. Bhat⁵⁰, V. Bhatnagar²⁸, G. Blazey⁵², S. Blessing⁴⁹, K. Bloom⁶⁷, A. Boehnlein⁵⁰, D. Boline⁶², T.A. Bolton⁵⁹, E.E. Boos³⁹, G. Borissov⁴³, T. Bose⁶², A. Brandt⁷⁸, R. Brock⁶⁵, G. Brooijmans⁷⁰, A. Bross⁵⁰, D. Brown¹⁹, X.B. Bu⁷, D. Buchholz⁵³, M. Buehler⁸¹, V. Buescher²⁵, V. Bunichev³⁹, S. Burdin^{43,c}, T.H. Burnett⁸², C.P. Buszello⁴⁴, P. Calfayan²⁶, B. Calpas¹⁵, S. Calvet¹⁶, J. Cammin⁷¹, M.A. Carrasco-Lizarraga³⁴, E. Carrera⁴⁹, W. Carvalho³, B.C.K. Casey⁵⁰, H. Castilla-Valdez³⁴, S. Chakrabarti⁷², D. Chakraborty⁵², K.M. Chan⁵⁵, A. Chandra⁴⁸, E. Cheu⁴⁶, D.K. Cho⁶², S.W. Cho³², S. Choi³³, B. Choudhary²⁹, T. Christoudias⁴⁴, S. Cihangir⁵⁰, D. Claes⁶⁷, J. Clutter⁵⁸, M. Cooke⁵⁰, W.E. Cooper⁵⁰, M. Corcoran⁸⁰, F. Couderc¹⁸, M.-C. Cousinou¹⁵, D. Cutts⁷⁷, M. Ćwiok³¹, A. Das⁴⁶, G. Davies⁴⁴, K. De⁷⁸, S.J. de Jong³⁶, E. De La Cruz-Burelo³⁴, K. DeVaughan⁶⁷, F. Déliot¹⁸, M. Demarteau⁵⁰, R. Demina⁷¹, D. Denisov⁵⁰, S.P. Denisov⁴⁰, S. Desai⁵⁰, H.T. Diehl⁵⁰, M. Diesburg⁵⁰, A. Dominguez⁶⁷, T. Dorland⁸², A. Dubey²⁹, L.V. Dudko³⁹, L. Duflot¹⁶, D. Duggan⁴⁹, A. Duperrin¹⁵, S. Dutt²⁸, A. Dyshkant⁵², M. Eads⁶⁷, D. Edmunds⁶⁵, J. Ellison⁴⁸, V.D. Elvira⁵⁰, Y. Enari⁷⁷, S. Eno⁶¹, M. Escalier¹⁵, H. Evans⁵⁴, A. Evdokimov⁷³, V.N. Evdokimov⁴⁰, G. Facini⁶³, A.V. Ferapontov⁷⁷, T. Ferbel^{61,71}, F. Fiedler²⁵, F. Filthaut³⁶, W. Fisher⁵⁰, H.E. Fisk⁵⁰, M. Fortner⁵², H. Fox⁴³, S. Fuess⁵⁰, T. Gadfort⁷⁰, C.F. Galea³⁶, A. Garcia-Bellido⁷¹, V. Gavrilov³⁸, P. Gay¹³, W. Geist¹⁹, W. Geng^{15,65}, C.E. Gerber⁵¹, Y. Gershtein^{49,b}, D. Gillberg⁶, G. Ginther^{50,71}, G. Golovanov³⁷, B. Gómez⁸, A. Goussiou⁸², P.D. Grannis⁷², S. Greder¹⁹, H. Greenlee⁵⁰, Z.D. Greenwood⁶⁰, E.M. Gregores⁴, G. Grenier²⁰, Ph. Gris¹³, J.-F. Grivaz¹⁶, A. Grohsjean¹⁸, S. Grünendahl⁵⁰, M.W. Grünewald³¹, F. Guo⁷², J. Guo⁷², G. Gutierrez⁵⁰, P. Gutierrez⁷⁵, A. Haas^{70,d}, P. Haefner²⁶, S. Hagopian⁴⁹, J. Haley⁶⁸, I. Hall⁶⁵, R.E. Hall⁴⁷, L. Han⁷, K. Harder⁴⁵, A. Harel⁷¹, J.M. Hauptman⁵⁷, J. Hays⁴⁴, T. Hebbeker²¹, D. Hedin⁵², J.G. Hegeman³⁵, A.P. Heinson⁴⁸, U. Heintz⁶², C. Hensel²⁴, I. Heredia-De La Cruz³⁴, K. Herner⁶⁴, G. Hesketh⁶³, M.D. Hildreth⁵⁵, R. Hirosky⁸¹, T. Hoang⁴⁹, J.D. Hobbs⁷², B. Hoeneisen¹², M. Hohlfeld²⁵, S. Hossain⁷⁵, P. Houben³⁵, Y. Hu⁷², Z. Hubacek¹⁰, N. Huske¹⁷, V. Hynek¹⁰, I. Iashvili⁶⁹, R. Illingworth⁵⁰, A.S. Ito⁵⁰, S. Jabeen⁶², M. Jaffré¹⁶, S. Jain⁷⁵, K. Jakobs²³, D. Jamin¹⁵, R. Jesik⁴⁴, K. Johns⁴⁶, C. Johnson⁷⁰, M. Johnson⁵⁰, D. Johnston⁶⁷, A. Jonckheere⁵⁰, P. Jonsson⁴⁴, A. Juste⁵⁰, E. Kajfasz¹⁵, D. Karmanov³⁹, P.A. Kasper⁵⁰, I. Katsanos⁶⁷, V. Kaushik⁷⁸, R. Kehoe⁷⁹, S. Kermiche¹⁵, N. Khalatyan⁵⁰, A. Khanov⁷⁶, A. Kharchilava⁶⁹, Y.N. Kharzheev³⁷, D. Khatidze⁷⁷, M.H. Kirby⁵³, M. Kirsch²¹, B. Klima⁵⁰, J.M. Kohli²⁸, J.-P. Konrath²³, A.V. Kozelov⁴⁰, J. Kraus⁶⁵, T. Kuhl²⁵, A. Kumar⁶⁹, A. Kupco¹¹, T. Kurča²⁰, V.A. Kuzmin³⁹, J. Kvita⁹, F. Lacroix¹³, D. Lam⁵⁵, S. Lammers⁵⁴, G. Landsberg⁷⁷, P. Lebrun²⁰, H.S. Lee³², W.M. Lee⁵⁰, A. Leflat³⁹, J. Lellouch¹⁷, L. Li⁴⁸, Q.Z. Li⁵⁰, S.M. Lietti⁵, J.K. Lim³², D. Lincoln⁵⁰, J. Linnemann⁶⁵, V.V. Lipaev⁴⁰, R. Lipton⁵⁰, Y. Liu⁷, Z. Liu⁶, A. Lobodenko⁴¹, M. Lokajicek¹¹, P. Love⁴³, H.J. Lubatti⁸², R. Luna-Garcia^{34,e}, A.L. Lyon⁵⁰, A.K.A. Maciel², D. Mackin⁸⁰, P. Mättig²⁷, R. Magaña-Villalba³⁴, P.K. Mal⁴⁶, S. Malik⁶⁷, V.L. Malyshev³⁷, Y. Maravin⁵⁹, B. Martin¹⁴, R. McCarthy⁷², C.L. McGivern⁵⁸, M.M. Meijer³⁶, A. Melnitchouk⁶⁶, L. Mendoza⁸, D. Menezes⁵², P.G. Mercadante⁴, M. Merkin³⁹, A. Meyer²¹, J. Meyer²⁴, N.K. Mondal³⁰, H.E. Montgomery⁵⁰, R.W. Moore⁶, T. Moulik⁵⁸, G.S. Muanza¹⁵, M. Mulhearn⁷⁰, O. Mundal²², L. Mundim³, E. Nagy¹⁵, M. Naimuddin⁵⁰, M. Narain⁷⁷, H.A. Neal⁶⁴, J.P. Negret⁸, P. Neustroev⁴¹, H. Nilsen²³, H. Nogima³, S.F. Novaes⁵, T. Nunnemann²⁶, G. Obrant⁴¹, C. Ochando¹⁶, D. Onoprienko⁵⁹, J. Orduna³⁴, N. Oshima⁵⁰, N. Osman⁴⁴, J. Osta⁵⁵, R. Otec¹⁰, G.J. Otero y Garzón¹, M. Owen⁴⁵, M. Padilla⁴⁸, P. Padley⁸⁰, M. Pangilinan⁷⁷, N. Parashar⁵⁶, S.-J. Park²⁴, S.K. Park³², J. Parsons⁷⁰, R. Partridge⁷⁷, N. Parua⁵⁴, A. Patwa⁷³, B. Penning²³, M. Perfilov³⁹, K. Peters⁴⁵, Y. Peters⁴⁵, P. Pétroff¹⁶, R. Piegaia¹, J. Piper⁶⁵, M.-A. Pleier⁷³, P.L.M. Podesta-Lerma^{34,f}, V.M. Podstavkov⁵⁰, Y. Pogorelov⁵⁵, M.-E. Pol², P. Polozov³⁸, A.V. Popov⁴⁰, M. Prewitt⁸⁰, S. Protopopescu⁷³, J. Qian⁶⁴, A. Quadt²⁴, B. Quinn⁶⁶, A. Rakitine⁴³, M.S. Rangel¹⁶, K. Ranjan²⁹, P.N. Ratoff⁴³, P. Renkel⁷⁹, P. Rich⁴⁵, M. Rijssenbeek⁷², I. Ripp-Baudot¹⁹, F. Rizatdinova⁷⁶, S. Robinson⁴⁴, M. Rominsky⁷⁵, C. Royon¹⁸, P. Rubinov⁵⁰, R. Ruchti⁵⁵, G. Safronov³⁸, G. Sajot¹⁴, A. Sánchez-Hernández³⁴, M.P. Sanders²⁶, B. Sanghi⁵⁰, G. Savage⁵⁰, L. Sawyer⁶⁰, T. Scanlon⁴⁴, D. Schaile²⁶, R.D. Schamberger⁷², Y. Scheglov⁴¹, H. Schellman⁵³, T. Schliephake²⁷, S. Schlobohm⁸², C. Schwanenberger⁴⁵,

R. Schwienhorst⁶⁵, J. Sekaric⁵⁸, H. Severini⁷⁵, E. Shabalina²⁴, M. Shamim⁵⁹, V. Shary¹⁸, A.A. Shchukin⁴⁰, R.K. Shivpuri²⁹, V. Siccaldi¹⁹, V. Simak¹⁰, V. Sirotenko⁵⁰, P. Skubic⁷⁵, P. Slattery⁷¹, D. Smirnov⁵⁵, G.R. Snow⁶⁷, J. Snow⁷⁴, S. Snyder⁷³, S. Söldner-Rembold⁴⁵, L. Sonnenschein²¹, A. Sopczak⁴³, M. Sosebee⁷⁸, K. Soustruznik⁹, B. Spurlock⁷⁸, J. Stark¹⁴, V. Stolin³⁸, D.A. Stoyanova⁴⁰, J. Strandberg⁶⁴, M.A. Strang⁶⁹, E. Strauss⁷², M. Strauss⁷⁵, R. Ströhmer²⁶, D. Strom⁵¹, L. Stutte⁵⁰, S. Sumowidagdo⁴⁹, P. Svoisky³⁶, M. Takahashi⁴⁵, A. Tanasijczuk¹, W. Taylor⁶, B. Tiller²⁶, M. Titov¹⁸, V.V. Tokmenin³⁷, I. Torchiani²³, D. Tsybychev⁷², B. Tuchming¹⁸, C. Tully⁶⁸, P.M. Tuts⁷⁰, R. Unalan⁶⁵, L. Uvarov⁴¹, S. Uvarov⁴¹, S. Uzunyan⁵², P.J. van den Berg³⁵, R. Van Kooten⁵⁴, W.M. van Leeuwen³⁵, N. Varelas⁵¹, E.W. Varnes⁴⁶, I.A. Vasilyev⁴⁰, P. Verdier²⁰, L.S. Vertogradov³⁷, M. Verzocchi⁵⁰, M. Vesterinen⁴⁵, D. Vilanova¹⁸, P. Vint⁴⁴, P. Vokac¹⁰, R. Wagner⁶⁸, H.D. Wahl⁴⁹, M.H.L.S. Wang⁷¹, J. Warchol⁵⁵, G. Watts⁸², M. Wayne⁵⁵, G. Weber²⁵, M. Weber^{50,g}, A. Wenger^{23,h}, M. Wetstein⁶¹, A. White⁷⁸, D. Wicke²⁵, M.R.J. Williams⁴³, G.W. Wilson⁵⁸, S.J. Wimpenny⁴⁸, M. Wobisch⁶⁰, D.R. Wood⁶³, T.R. Wyatt⁴⁵, Y. Xie⁷⁷, C. Xu⁶⁴, S. Yacoub⁵³, R. Yamada⁵⁰, W.-C. Yang⁴⁵, T. Yasuda⁵⁰, Y.A. Yatsunencko³⁷, Z. Ye⁵⁰, H. Yin⁷, K. Yip⁷³, H.D. Yoo⁷⁷, S.W. Youn⁵⁰, J. Yu⁷⁸, C. Zeitnitz²⁷, S. Zelitch⁸¹, T. Zhao⁸², B. Zhou⁶⁴, J. Zhu⁷², M. Zielinski⁷¹, D. Zieminska⁵⁴, L. Zivkovic⁷⁰, V. Zutshi⁵², and E.G. Zverev³⁹

(The DØ Collaboration)

¹Universidad de Buenos Aires, Buenos Aires, Argentina

²LAFEX, Centro Brasileiro de Pesquisas Físicas, Rio de Janeiro, Brazil

³Universidade do Estado do Rio de Janeiro, Rio de Janeiro, Brazil

⁴Universidade Federal do ABC, Santo André, Brazil

⁵Instituto de Física Teórica, Universidade Estadual Paulista, São Paulo, Brazil

⁶University of Alberta, Edmonton, Alberta, Canada; Simon Fraser University, Burnaby, British Columbia, Canada; York University, Toronto, Ontario, Canada and McGill University, Montreal, Quebec, Canada

⁷University of Science and Technology of China, Hefei, People's Republic of China

⁸Universidad de los Andes, Bogotá, Colombia

⁹Center for Particle Physics, Charles University,

Faculty of Mathematics and Physics, Prague, Czech Republic

¹⁰Czech Technical University in Prague, Prague, Czech Republic

¹¹Center for Particle Physics, Institute of Physics, Academy of Sciences of the Czech Republic, Prague, Czech Republic

¹²Universidad San Francisco de Quito, Quito, Ecuador

¹³LPC, Université Blaise Pascal, CNRS/IN2P3, Clermont, France

¹⁴LPSC, Université Joseph Fourier Grenoble 1, CNRS/IN2P3, Institut National Polytechnique de Grenoble, Grenoble, France

¹⁵CPPM, Aix-Marseille Université, CNRS/IN2P3, Marseille, France

¹⁶LAL, Université Paris-Sud, IN2P3/CNRS, Orsay, France

¹⁷LPNHE, IN2P3/CNRS, Universités Paris VI and VII, Paris, France

¹⁸CEA, Irfu, SPP, Saclay, France

¹⁹IPHC, Université de Strasbourg, CNRS/IN2P3, Strasbourg, France

²⁰IPNL, Université Lyon 1, CNRS/IN2P3, Villeurbanne, France and Université de Lyon, Lyon, France

²¹III. Physikalisches Institut A, RWTH Aachen University, Aachen, Germany

²²Physikalisches Institut, Universität Bonn, Bonn, Germany

²³Physikalisches Institut, Universität Freiburg, Freiburg, Germany

²⁴II. Physikalisches Institut, Georg-August-Universität Göttingen, Göttingen, Germany

²⁵Institut für Physik, Universität Mainz, Mainz, Germany

²⁶Ludwig-Maximilians-Universität München, München, Germany

²⁷Fachbereich Physik, University of Wuppertal, Wuppertal, Germany

²⁸Panjab University, Chandigarh, India

²⁹Delhi University, Delhi, India

³⁰Tata Institute of Fundamental Research, Mumbai, India

³¹University College Dublin, Dublin, Ireland

³²Korea Detector Laboratory, Korea University, Seoul, Korea

³³SungKyunKwan University, Suwon, Korea

³⁴CINVESTAV, Mexico City, Mexico

³⁵FOM-Institute NIKHEF and University of Amsterdam/NIKHEF, Amsterdam, The Netherlands

³⁶Radboud University Nijmegen/NIKHEF, Nijmegen, The Netherlands

³⁷Joint Institute for Nuclear Research, Dubna, Russia

³⁸Institute for Theoretical and Experimental Physics, Moscow, Russia

³⁹Moscow State University, Moscow, Russia

- ⁴⁰*Institute for High Energy Physics, Protvino, Russia*
⁴¹*Petersburg Nuclear Physics Institute, St. Petersburg, Russia*
⁴²*Stockholm University, Stockholm, Sweden, and Uppsala University, Uppsala, Sweden*
⁴³*Lancaster University, Lancaster, United Kingdom*
⁴⁴*Imperial College, London, United Kingdom*
⁴⁵*University of Manchester, Manchester, United Kingdom*
⁴⁶*University of Arizona, Tucson, Arizona 85721, USA*
⁴⁷*California State University, Fresno, California 93740, USA*
⁴⁸*University of California, Riverside, California 92521, USA*
⁴⁹*Florida State University, Tallahassee, Florida 32306, USA*
⁵⁰*Fermi National Accelerator Laboratory, Batavia, Illinois 60510, USA*
⁵¹*University of Illinois at Chicago, Chicago, Illinois 60607, USA*
⁵²*Northern Illinois University, DeKalb, Illinois 60115, USA*
⁵³*Northwestern University, Evanston, Illinois 60208, USA*
⁵⁴*Indiana University, Bloomington, Indiana 47405, USA*
⁵⁵*University of Notre Dame, Notre Dame, Indiana 46556, USA*
⁵⁶*Purdue University Calumet, Hammond, Indiana 46323, USA*
⁵⁷*Iowa State University, Ames, Iowa 50011, USA*
⁵⁸*University of Kansas, Lawrence, Kansas 66045, USA*
⁵⁹*Kansas State University, Manhattan, Kansas 66506, USA*
⁶⁰*Louisiana Tech University, Ruston, Louisiana 71272, USA*
⁶¹*University of Maryland, College Park, Maryland 20742, USA*
⁶²*Boston University, Boston, Massachusetts 02215, USA*
⁶³*Northeastern University, Boston, Massachusetts 02115, USA*
⁶⁴*University of Michigan, Ann Arbor, Michigan 48109, USA*
⁶⁵*Michigan State University, East Lansing, Michigan 48824, USA*
⁶⁶*University of Mississippi, University, Mississippi 38677, USA*
⁶⁷*University of Nebraska, Lincoln, Nebraska 68588, USA*
⁶⁸*Princeton University, Princeton, New Jersey 08544, USA*
⁶⁹*State University of New York, Buffalo, New York 14260, USA*
⁷⁰*Columbia University, New York, New York 10027, USA*
⁷¹*University of Rochester, Rochester, New York 14627, USA*
⁷²*State University of New York, Stony Brook, New York 11794, USA*
⁷³*Brookhaven National Laboratory, Upton, New York 11973, USA*
⁷⁴*Langston University, Langston, Oklahoma 73050, USA*
⁷⁵*University of Oklahoma, Norman, Oklahoma 73019, USA*
⁷⁶*Oklahoma State University, Stillwater, Oklahoma 74078, USA*
⁷⁷*Brown University, Providence, Rhode Island 02912, USA*
⁷⁸*University of Texas, Arlington, Texas 76019, USA*
⁷⁹*Southern Methodist University, Dallas, Texas 75275, USA*
⁸⁰*Rice University, Houston, Texas 77005, USA*
⁸¹*University of Virginia, Charlottesville, Virginia 22901, USA and*
⁸²*University of Washington, Seattle, Washington 98195, USA*
(Dated: September 25, 2009)

We present a direct measurement of the width of the W boson using the shape of the transverse mass distribution of $W \rightarrow e\nu$ candidates selected in 1 fb^{-1} of data collected with the D0 detector at the Fermilab Tevatron collider in $p\bar{p}$ collisions at $\sqrt{s} = 1.96 \text{ TeV}$. We use the same methods and data sample that were used for our recently published W boson mass measurement, except for the modeling of the recoil, which is done with a new method based on a recoil library. Our result, $2.028 \pm 0.072 \text{ GeV}$, is in agreement with the predictions of the standard model and is the most precise direct measurement result from a single experiment to date.

PACS numbers: 14.70.Fm, 13.38.Be, 13.85.Qk

The gauge structure of the standard model (SM) of electromagnetic, weak, and strong interactions tightly constrains the properties and interactions of the carriers of these forces, the gauge bosons. Any departure from its predictions would be an indication of physics beyond the SM. The W boson is one of the carriers of the weak

force and has a predicted decay width of

$$\Gamma_W = (3 + 2f_{QCD}) \frac{G_F M_W^3}{6\sqrt{2}\pi} (1 + \delta), \quad (1)$$

where G_F is the Fermi coupling constant, M_W is the mass of the W boson and $f_{QCD} = 3(1 + \alpha_s(M_W^2)/\pi)$ is a QCD correction factor given in the first order of the

strong coupling constant α_s . The radiative correction δ is calculated to be 2.1% with an uncertainty that is less than 0.5% in the SM [1]. Current world average values for G_F [2] and M_W [3] predict $\Gamma_W = 2.093 \pm 0.002$ GeV. Physics beyond the SM, such as new heavy particles that couple to the W boson, could alter the higher order vertex corrections that enter into δ and modify Γ_W [4].

Direct measurements of Γ_W have been previously performed by the CDF and D0 collaborations [5–8]. The width has also been measured at the CERN LEP e^+e^- collider [9]. The combined Tevatron average is $\Gamma_W = 2.056 \pm 0.062$ GeV, and the current world average is $\Gamma_W = 2.106 \pm 0.050$ GeV [5].

We present a direct measurement of Γ_W using the shape of the transverse mass (M_T) distribution of $W \rightarrow e\nu$ candidates from $p\bar{p}$ collisions with center-of-mass energy of 1.96 TeV using 1 fb^{-1} of collisions collected by the D0 detector [10]. The transverse mass is defined as $M_T = \sqrt{2p_T^e p_T^\nu [1 - \cos(\Delta\phi)]}$, where $\Delta\phi$ is the opening angle between the electron and neutrino, and p_T^e and p_T^ν are the transverse momenta of the electron and neutrino respectively. The fraction of events with large M_T is sensitive to Γ_W , although it is also influenced by the detector responses to the electron and the hadronic recoil. We use a new data-driven method for modeling the hadronic recoil of the W boson using a recoil library of Z boson candidates [11]. The method for extracting Γ_W is similar to that described in a recent Letter on a measurement of W boson mass by the D0 collaboration [12].

The D0 detector includes a central tracking system, composed of a silicon microstrip tracker (SMT) and a central fiber tracker, both located within a 2 T superconducting solenoidal magnet and optimized for tracking capability for $|\eta_D| \leq 3$ [13]. Three uranium and liquid argon calorimeters provide coverage for $|\eta_D| \leq 4.2$: a central calorimeter (CC) covering $|\eta_D| \leq 1.1$, and two end-cap calorimeters (EC) with a coverage of $1.5 \leq |\eta_D| \leq 4.2$ for jets and $1.5 \leq |\eta_D| \leq 3.2$ for electrons. In addition to the preshower detectors, scintillators between the CC and EC cryostats provide sampling of developing showers at $1.1 \leq |\eta_D| \leq 1.5$. A muon system surrounds the calorimetry and consists of three layers of scintillators and drift tubes, and a 1.8 T iron toroid with a coverage of $|\eta_D| \leq 2$.

The analysis uses $W \rightarrow e\nu$ candidates for the width extraction and $Z \rightarrow ee$ candidates to tune the simulation of the detector response used in the extraction of the W boson width from data. The data sample was collected using a set of inclusive single-electron triggers. The position of the reconstructed vertex of the hard collision along the beam line is required to be within 60 cm of the center of the detector. Throughout this Letter we use “electron” to imply either electron or positron.

Electron candidates are required to have $p_T^e > 25$ GeV and must be spatially matched to a reconstructed track in the central tracking system. We calculate p_T^e using the

energy from the calorimeter and angles from the matched track. The track must have at least one SMT hit and $p_T > 10$ GeV. Electron candidates are further required to pass shower shape and energy isolation requirements and to be in the fiducial region of the CC calorimeter.

p_T^ν is inferred from the observed missing transverse energy, \cancel{E}_T , reconstructed from \vec{p}_T^e and the transverse momentum of the hadronic recoil (\vec{u}_T) using $\vec{\cancel{E}}_T = -[\vec{p}_T^e + \vec{u}_T]$. The recoil vector \vec{u}_T is the vector sum of energies in calorimeter cells outside those cells used for defining the electron. The recoil is a mixture of the “hard” recoil that balances the boson transverse momentum and “soft” contributions from particles produced by the spectator quarks, other $p\bar{p}$ collisions in the same beam crossing, electronics noise, and residual energy in the detector from previous beam crossings.

W boson candidate events are required to have a CC electron with $p_T^e > 25$ GeV, $\cancel{E}_T > 25$ GeV, $u_T < 15$ GeV, and $50 < M_T < 200$ GeV. Z boson candidate events are required to have two CC electrons with $p_T^e > 25$ GeV and $u_T < 15$ GeV. These selections yield 499,830 W boson candidates (5,272 candidates with $100 < M_T < 200$ GeV) and 18,725 Z boson candidates with the invariant mass (M_{ee}) of the two electrons between 70 and 110 GeV.

The W boson width is extracted by comparing the M_T data distribution with distributions in simulated templates generated at different width values. The prediction (in number of events) of signal-plus-background is normalized to the data in the $50 < M_T < 100$ GeV window. A binned negative log-likelihood method is used to extract Γ_W in the range $100 < M_T < 200$ GeV.

There are two main sources of events with high M_T : events that truly contain a high mass W boson, and events with a W boson whose mass is close to the W boson mass central value but are produced with large u_T . This second category of events can be mis-reconstructed at high M_T because of resolution effects and also because the magnitude of the recoil vector is systematically underestimated due to the response of the calorimeter to low energy hadrons, energy thresholds on the calorimeter energies, and magnetic field effects.

Another experimental challenge arises from the p_T dependence of the electron identification efficiency, which can alter the shape of the M_T distribution. The electron isolation requirement used in this analysis has a non-negligible dependence on the electron p_T which is measured using a detailed GEANT-based Monte Carlo (MC) simulation [14] and tested using $Z \rightarrow ee$ events.

A fast MC simulation is used for the production of the M_T templates. W and Z boson production and decay properties are modeled by the RESBOS event generator [15] interfaced with PHOTOS [16]. RESBOS uses gluon resummation at low boson p_T and a next-to-leading order perturbative QCD calculation at high boson p_T . The CTEQ6.1M parton distribution functions (PDFs) [17]

are used. PHOTOS is used for simulation of final state radiation (FSR). Photons and electrons that are nearly collinear are merged using an algorithm that mimics the calorimeter clustering algorithm.

The detector response and resolution for electrons and photons are simulated using a parameterization based on collider data control samples, a detailed GEANT-based simulation of the detector, and external constraints, such as the precise measurement of the Z boson mass from the LEP experiments [18]. The primary control sample is $Z \rightarrow ee$ events, although $W \rightarrow e\nu$ events are also used in a limited way. The modeling of the electron energy response, resolution and selection efficiencies is described in detail in [12]. The number of Z boson candidates in data sets the scale for the systematic uncertainties related to the electron modeling in the simulation, which are listed in detail in Table I.

The modeling of the recoil is based on the recoil library obtained from $Z \rightarrow ee$ events [11]. A Bayesian unsmearing procedure [19] allows the transformation of the two-dimensional distribution of reconstructed Z boson \vec{p}_T and the measured recoil momentum \vec{u}_T to one between the true Z boson \vec{p}_T and the measured recoil \vec{u}_T . For each simulated $W \rightarrow e\nu$ event with a generator-level transverse momentum value \vec{p}_T , we select \vec{u}_T randomly from the Z boson recoil library with the same value of \vec{p}_T . The uncertainty on the recoil system simulation from this method is dominated by the limited statistics of the Z boson sample; other systematic uncertainties originate from the modeling of FSR photons, acceptance differences between W and Z boson events, corrections for underlying energy beneath the electron cluster, residual efficiency-related correlations between the electron and the recoil system, and the unfolding procedure. Previous M_W and Γ_W measurements have relied upon parameterizations of the recoil kinematics based on phenomenological models of the recoil and detector response. The library method used here includes the actual detector response for the hadronic recoil and also the correlations between different components of the hadronic recoil. This method does not rely on the GEANT-based simulation of the recoil system and does not have any tunable parameters. The overall systematic uncertainty on Γ_W due to the recoil model is found to be 41 MeV [11].

The backgrounds to $W \rightarrow e\nu$ events are (a) $Z \rightarrow ee$ events in which one electron is not detected; (b) multijet production in which one jet is misidentified as an electron and mis-measurement of the hadronic activity in the event leads to apparent \cancel{E}_T ; (c) $W \rightarrow \tau\nu \rightarrow e\nu\nu\nu$ events. The $Z \rightarrow ee$ background arises mainly when one of the two electrons is in the region between the CC and EC calorimeters. It is estimated from events with one electron with a high- p_T track opposite in azimuth pointing towards the gap. The estimated background fraction is $(0.90 \pm 0.01)\%$ for $50 < M_T < 200$ GeV. The background fraction from multijet events is estimated from a loose

sample of candidate events without track match requirements and then selecting a subset of events which satisfy the final tighter track match requirement. From $Z \rightarrow ee$ events, and a sample of multijet events passing the pre-selection but with low \cancel{E}_T , we determine the probabilities with which real and misidentified electrons will pass the track match requirement. These two probabilities, along with the numbers of events selected in the loose and tight samples allow us to calculate the fraction of multijet events in the dataset. The background contamination from multijet events is estimated to be $(1.49 \pm 0.03)\%$ for $50 < M_T < 200$ GeV. The $W \rightarrow \tau\nu \rightarrow e\nu\nu\nu$ background is determined using a GEANT-based simulation to be $(1.60 \pm 0.02)\%$ for $50 < M_T < 200$ GeV and is normalized to the $W \rightarrow e\nu$ events in the same simulation. The overall background fraction is found to be $(4.36 \pm 0.05)\%$ with M_T between 100 and 200 GeV. The uncertainties on the normalization and shape of the backgrounds cause a 6 MeV systematic uncertainty on Γ_W .

The systematic uncertainties in the determination of the W boson width are due to effects that could alter the M_T distribution. Uncertainties in the parameters of the fast MC simulation can affect the measurement of Γ_W . To estimate the effects, we allow these parameters to vary by one standard deviation and regenerate the M_T templates. Systematic uncertainties resulting from the boson p_T spectrum are evaluated by varying the g_2 parameter of the RESBOS nonperturbative prescription within the uncertainties obtained from a global fit [20] and propagating them to the W boson width. Systematic uncertainties due to the PDFs are evaluated using the prescription given by the CTEQ collaboration [17]. Systematic uncertainties from the modeling of electroweak radiative corrections are obtained by comparisons with WGRAD [21] and ZGRAD2 [22]. The systematic uncertainty due to the M_W uncertainty is obtained by varying the input M_W by ± 23 MeV [3]. Systematic uncertainties on Γ_W due to these sources are listed in Table I.

We fit the M_T data distribution to a set of templates generated with an input W boson mass of 80.419 GeV at different assumed widths between a lower M_T value and $M_T = 200$ GeV. The lower M_T cut is varied from 90 to 110 GeV to demonstrate the stability of the fitted result. While the statistical uncertainty decreases as the lower M_T cut is reduced, the systematic uncertainty increases. The lowest overall uncertainty is obtained for a lower M_T cut of 100 GeV yielding $\Gamma_W = 2.028 \pm 0.039$ (stat) ± 0.061 (syst) GeV. The M_T distributions for the data and the MC template with backgrounds for the best fit value are shown in Fig. 1, which also shows the bin-by-bin χ values defined as the difference between the data and the template divided by the data statistical uncertainty. The detailed breakdown of the systematic uncertainties is summarized in Table I.

The methodology used to extract the width in this Letter is tested using W and Z boson events produced by

Source	$\Delta\Gamma_W$ (MeV)
Electron response model	33
Electron resolution model	10
Hadronic recoil model	41
Electron efficiencies	19
Backgrounds	6
PDF	20
Electroweak radiative corrections	7
Boson p_T	1
M_W	5
Total Systematic	61

TABLE I: Systematic uncertainties on the measurement of Γ_W .

a PYTHIA/GEANT-based simulation and the same analysis methods used for the data. The fast MC simulation is separately tuned for this study. Good agreement is found between the fitted Γ_W value and the input Γ_W value within the statistical precision of the test.

The Γ_W result obtained using the M_T spectrum is in agreement with the predictions of the SM. We get consistent values of the W boson width from fits to the p_T^e distribution (2.012 ± 0.046 (stat) GeV) and the \cancel{E}_T distribution (2.058 ± 0.036 (stat) GeV). The width can also be estimated directly from the fraction of events with $M_T > 100$ GeV, and this gives $\Gamma_W = 2.020 \pm 0.040$ (stat) GeV. The results are stable within errors when the data sample is divided into different regions of instantaneous Tevatron luminosity, run epoch, and different restrictions on u_T , electron η_D , $\vec{u}_T \cdot \hat{p}_T(e)$ and fiducial cuts on electron azimuthal angle.

As a further cross check of the recoil library method we also use it to measure the W boson mass using the M_T distribution over the region $65 < M_T < 90$ GeV. A value of $M_W = 80.404 \pm 0.023$ (stat) ± 0.038 (syst) GeV is found, in good agreement with the result, $M_W = 80.401 \pm 0.023$ (stat) ± 0.037 (syst) GeV, obtained using the same data set and the parameterized recoil model [12].

In conclusion, we have presented a new direct measurement of the width of the W boson using 1 fb^{-1} of data collected by the D0 detector at the Tevatron collider. A method to simulate the recoil system in $W \rightarrow e\nu$ events using a recoil library built from $Z \rightarrow ee$ events is used for the first time. Our result, $\Gamma_W = 2.028 \pm 0.072$ GeV, is in agreement with the prediction of the SM and is the most precise direct measurement result from a single experiment to date.

We thank the staffs at Fermilab and collaborating institutions, and acknowledge support from the DOE and NSF (USA); CEA and CNRS/IN2P3 (France); FASI, Rosatom and RFBR (Russia); CNPq, FAPERJ, FAPESP and FUNDUNESP (Brazil); DAE and DST (India); Colciencias (Colombia); CONACyT (Mexico); KRF and KOSEF (Korea); CONICET and UBACyT (Argentina); FOM (The Netherlands); STFC and the Royal

Society (United Kingdom); MSMT and GACR (Czech Republic); CRC Program, CFI, NSERC and WestGrid Project (Canada); BMBF and DFG (Germany); SFI (Ireland); The Swedish Research Council (Sweden); Graduate Research Board, University of Maryland (USA); and CAS and CNSF (China).

- [a] Visitor from Augustana College, Sioux Falls, SD, USA.
[b] Visitor from Rutgers University, Piscataway, NJ, USA.
[c] Visitor from The University of Liverpool, Liverpool, UK.
[d] Visitor from SLAC, Menlo Park, CA, USA.
[e] Visitor from Centro de Investigacion en Computacion - IPN, Mexico City, Mexico.
[f] Visitor from ECFM, Universidad Autonoma de Sinaloa, Culiacán, Mexico.
[g] Visitor from Universität Bern, Bern, Switzerland.
[h] Visitor from Universität Zürich, Zürich, Switzerland.
- [1] J.L. Rosner, M.P. Worah, and T. Takeuchi, Phys. Rev. D **49**, 1363 (1994).
[2] C. Amsler *et al.* (Particle Data Group), Phys. Lett. B **667**, 1 (2008).
[3] The Tevatron Electroweak Working Group (CDF and D0 Collaborations), arXiv:0908.1374 [hep-ex] (2009).
[4] V. Barger *et al.*, Phys. Rev. D **28**, 2912 (1983); M. Drees, C.S. Kim, and X. Tata, Phys. Rev. D **37**, 784 (1988).
[5] F. Abe *et al.* (CDF Collaboration), Phys. Rev. Lett. **85**, 3347 (2000).
[6] T. Aaltonen *et al.* (CDF Collaboration), Phys. Rev. Lett. **100**, 071801 (2008).
[7] V.M. Abazov *et al.* (D0 Collaboration), Phys. Rev. D **66**, 032008 (2002).
[8] V.M. Abazov *et al.* (CDF and D0 Collaborations), Phys. Rev. D **70**, 092008 (2004).
[9] S. Schael *et al.* (ALEPH Collaboration), Eur. Phys. J. C **47**, 309 (2006); G. Abbiendi *et al.* (OPAL Collaboration), Eur. Phys. J. C **45**, 307 (2006); P. Achard *et al.* (L3 Collaboration), Eur. Phys. J. C **45**, 569 (2006); P. Abreu *et al.* (DELPHI Collaboration), Phys. Lett. B **511**, 159 (2001).
[10] V.M. Abazov *et al.* (D0 Collaboration), Nucl. Instrum. Methods A **565**, 463 (2006).
[11] V.M. Abazov *et al.* (D0 Collaboration), arXiv:0907.3713 [hep-ex] (2009), Nucl. Instrum. Methods A (to be published).
[12] V.M. Abazov *et al.* (D0 Collaboration), arXiv:0908.0766 [hep-ex] (2009), Phys. Rev. Lett. (to be published).
[13] The polar angle θ is defined with respect to the positive z axis, which is defined along the proton beam direction. Pseudorapidity is defined as $\eta = -\ln[\tan(\theta/2)]$. η_D is the pseudorapidity measured with respect to the center of the detector.
[14] R. Brun and F. Carminati, CERN Program Library Long Writeup W5013, 1993 (unpublished).
[15] C. Balazs and C.P. Yuan, Phys. Rev. D **56**, 5558 (1997).
[16] E. Barberio and Z. Was, Comput. Phys. Commun **79**, 291 (1994); we use PHOTOS version 2.0.
[17] J. Pumplin *et al.*, J. High Energy Phys. **07** (2002) 012.
[18] C. Amsler *et al.*, Phys. Lett. B **667**, 1 (2008) and references therein.

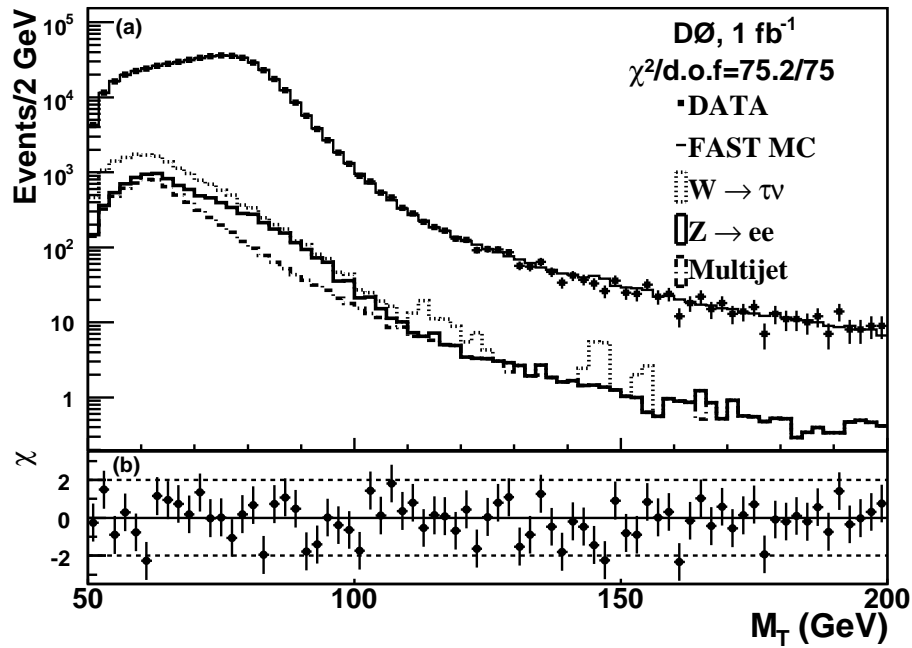


FIG. 1: Comparison of the M_T data distribution with its expectation from a fast MC simulation of $W \rightarrow e\nu$ events to which smaller backgrounds have been added (a); χ values for each M_T bin (b). The measured Γ_W value is used for the fast MC prediction. The distribution of the fast MC simulation, including the cumulative contributions of the different backgrounds, is normalized to the data in the region $50 < M_T < 100$ GeV.

[19] G. D'Agostini, Nucl. Instrum. Methods A **362**, 487 (1995).

[20] F. Landry *et al.*, Phys. Rev. D **67**, 073016 (2003).

[21] U. Baur, S. Keller, and D. Wackerth, Phys. Rev. D **59**, 013002 (1999).

[22] U. Baur, S. Keller, and W.K. Sakumoto, Phys. Rev. D **57**, 199 (1998); U. Baur *et al.*, Phys. Rev. D **65**, 033007 (2002).